Journal of Photochemistry and Photobiology A: Chemistry 306 (2015) 13–20

Contents lists available at ScienceDirect

Journal of Photochemistry and Photobiology A: Chemistry

journal homepage: www.elsevier.com/locate/jphotochem

$CBrF_3$ (Halon-1301): UV absorption spectrum between 210 and 320 K, atmospheric lifetime, and ozone depletion potential

François Bernard [a,b], Max R. McGillen [a,b], Eric L. Fleming [c,d], Charles H. Jackman [c], James B. Burkholder [a,*]

[a] National Oceanic and Atmospheric Administration (NOAA), Earth Systems Research Laboratory, Chemical Sciences Division, Department of Commerce, Boulder, CO, USA
[b] Cooperative Institute for Research in Environmental Sciences, University of Colorado, Boulder, CO, USA
[c] NASA Goddard Space Flight Center, Greenbelt, MD, USA
[d] Science Systems and Applications, Inc. Lanham, MD, USA

ARTICLE INFO

Article history:
Received 9 February 2015
Received in revised form 9 March 2015
Accepted 16 March 2015
Available online 17 March 2015

Keywords:
Bromotrifluoromethane
ozone depletion potential
UV absorption spectrum
temperature dependence
photolysis lifetime

ABSTRACT

$CBrF_3$ (Halon-1301) is a man-made ozone depleting substance that is a major source of bromine in the Earth's stratosphere. Halon-1301 is predominantly removed from the atmosphere by UV photolysis in the stratosphere at wavelengths between 200 and 225 nm. The existing level of uncertainty in the Halon-1301 UV absorption spectrum temperature-dependence directly impacts the ability to model stratospheric ozone chemistry and climate change. In this work, the UV absorption spectrum of Halon-1301 between 195 and 235 nm was measured over the temperature range 210–320 K. An empirical parameterization of the spectrum and its temperature dependence is presented. The present results are critically compared with results from previous studies and the current recommendation for use in atmospheric models. A global annually averaged lifetime for Halon-1301 of 74.6 (73.7–75.5) years was calculated using a 2-D atmospheric model and the present results. The range of lifetimes given in parenthesis represents the possible values due solely to the 2σ uncertainty in the Halon-1301 UV spectrum obtained in this work. In addition, the $CBrF_3$ ozone depletion potential was calculated using the 2-D model to be 18.6 ($\pm$0.1) using the UV spectrum and 2σ uncertainty from this work.

Published by Elsevier B.V.

1. Introduction

$CBrF_3$ (Halon-1301) is an atmospherically long-lived ozone depleting substance of anthropogenic origin; it is used commercially as a fire suppressant and explosion prevention agent. The currently recommended atmospheric lifetime of Halon-1301 is 77.4 years [1]. Halon-1301 is a major source of stratospheric bromine, which is more efficient than chlorine in the depletion of stratospheric ozone [2]. The ozone depletion potential (ODP) (see WMO [2] for ODP definition) of Halon-1301 was estimated to be 15.9, which is the highest among all halocarbons [2]. Halon-1301 has been amended within the Montreal protocol to stop its production and commercialization. In the present atmosphere, the mixing ratio of $CBrF_3$ is increasing, although the rate of increase declined between 2005 and 2008 compared to 2003–2004 [2]. The Halon-1301 mixing ratio was 3.3 ppt in 2012, which represents an increase from 2.5 ppt in 1996 [3], while the total stratospheric bromine mixing ratio was ~22 ppt in 2008 [2]. Future projections indicate that $CBrF_3$ will be the largest contributor to total tropospheric bromine after 2024 and account for more than 80% of the total bromine by 2060 [2–4]. In addition to measurements of the atmospheric abundance of $CBrF_3$, atmospheric modeling of the impact of $CBrF_3$ on stratospheric ozone and climate change requires an accurate understanding of its atmospheric loss processes.

Halon-1301 is predominantly removed from the atmosphere by UV photolysis in the stratosphere with $O(^1D)$ reactive loss making a minor (~0.7%) contribution to the total loss. Halon-1301 photolysis in the troposphere represents a minor loss process, ~0.2% [1]. Stratospheric photolysis of $CBrF_3$ occurs primarily in the short wavelength region with wavelengths between 190 and 230 nm accounting for 99.8% of its total photolysis rate [1]. Numerous studies have reported absorption spectra of $CBrF_3$, where the agreement within the 190–230 nm wavelength region [5] among the room temperature studies is ~10%, or better. Two of these studies included the temperature dependence of the $CBrF_3$ spectrum, Gillotay and Simon [6] (168–280 nm, 210–295 K) and Burkholder et al. [7] (190–260 nm, 210–296 K). Although the room

* Corresponding author. Tel.: +1 303 497 3252; fax: +1 303 497 5822.
E-mail address: james.b.burkholder@noaa.gov (J.B. Burkholder).

http://dx.doi.org/10.1016/j.jphotochem.2015.03.012
1010-6030/Published by Elsevier B.V.

temperature spectra from these two studies agree, to within ~5%, significant differences in the reported spectrum temperature dependence over the critical wavelength region exist between these datasets. The transition peaking near 205 nm is most likely due to a $\sigma^* \leftarrow n$ electronic transition, $(C—Br)^* \leftarrow Br$ transition [8]. The $CBrF_3$ spectrum wavelength and temperature dependence parameterization reported in Burkholder et al. [7] was recommended in SPARC [1] for use in atmospheric models, although an uncertainty of ~20% was assigned to the 190–230 nm wavelength region to account for the discrepancies in the experimental data for the temperature dependence of the $CBrF_3$ spectrum [1]. Because of the importance of $CBrF_3$ to stratospheric ozone chemistry, further laboratory studies designed to reduce the uncertainty in the $CBrF_3$ UV spectrum temperature dependence are warranted.

In this work, the UV absorption spectrum, $\sigma(\lambda,T)$, of Halon-1301 was measured between 195 and 235 nm over the temperature range 210–320 K and the obtained results are compared with previously reported spectra. A $\sigma(\lambda,T)$ parameterization of the present data for use in atmospheric models is presented. The impact of the $\sigma(\lambda,T)$ data, including its estimated uncertainty, obtained in this work on the lifetime and ODP of $CBrF_3$ was evaluated using the Goddard Space Flight Center (GSFC) 2-D atmospheric model [9,10].

2. Experimental details

The apparatus used in this work has been described in detail in previous studies from this laboratory [11,12] and is described only briefly here. The experimental apparatus consisted of a 30 W D_2 lamp, a jacketed single pass absorption cell with a 90.4 cm pathlength, a 0.25 m monochromator with a photomultiplier tube detector. The monochromator wavelength was calibrated using an Hg Pen-Ray lamp (±0.05 nm). The temperature of the absorption cell was maintained by circulating a temperature-regulated fluid through its jacket. The fluid temperature was measured (±0.5 K) using thermocouples in the circulating bath and at the exit of the cell. The temperature gradient along the length of the absorption cell was estimated to be ~0.5 K for temperatures ≥263 K and ~1 K for temperatures ≤250 K [13].

Absorption cross sections were obtained using Beer's law

$$A(\lambda) = -\ln\left[\frac{I(\lambda)}{I_0(\lambda)}\right] = \sigma(\lambda,T) \times L \times [\text{Halon} - 1301] \quad (1)$$

where $A(\lambda)$ is the absorbance at wavelength λ, $I(\lambda)$ and $I_0(\lambda)$ are the measured light intensities in the presence or in the absence of sample, respectively, $\sigma(\lambda,T)$ is the absorption cross section at temperature T, L is the optical pathlength in the absorption cell, and [Halon-1301] is the concentration of Halon-1301 in the absorption cell. All absorption measurements were performed under static conditions. Gas-phase UV absorption cross sections were determined at 9 discrete wavelengths between 195 and 235 nm (5 nm intervals) and at 6 temperatures between 210 and 320 K. The concentration of $CBrF_3$ was determined from the measured cell pressure and the ideal gas law. $I(\lambda)$ and the cell pressure were recorded continuously with a sampling rate of 1 kHz. The minimum and maximum $CBrF_3$ mixture pressure depended on the measurement wavelength and was chosen such that the minimum absorbance was >0.015 and the maximum absorbance was ~1.0, if possible. $\sigma(\lambda,T)$ was determined from a linear least-squares fit of $A(\lambda)$ vs. $[CBrF_3]$ with at least ten different concentrations of $CBrF_3$ were included in the fit.

3. Materials

Two different $CBrF_3$ samples with stated purities of >99% (#1) and 99% (#2) were used over the course of this study. He (UHP, 99.999%) was used in the preparation of sample mixtures and to flush the absorption cell. Gas mixtures were prepared manometrically in 12 L Pyrex bulbs; samples with 2.13 and 5.33% (#1) and 5.31% (#2) mixing ratios were used. For the 5.33% and 5.31% mixtures, the Halon sample was purified using several freeze-pump-thaw cycles before preparing the gas mixtures. Infrared spectra of the Halon-1301 mixtures were recorded using a Fourier transform infrared spectrometer and found to be in good agreement, to within ±1–2%, with the spectrum reported in the Pacific Northwest National Laboratory infrared database [14]. Pressures were measured using 100 and 1000 Torr capacitance manometers. Quoted uncertainties throughout this paper are 2σ unless stated otherwise.

4. Results and discussion

In this section, the $CBrF_3$ UV absorption cross sections obtained in this work are presented along with an uncertainty analysis. A spectrum parameterization, useful for atmospheric model calculations, that reproduces our $\sigma(\lambda,T)$ data to within the measurement precision is also presented. Our results are critically compared with results from previous studies as well as the recommendations given in Sander et al. [5]. The atmospheric impact of the present results is presented in the Atmospheric Implications section.

4.1. $CBrF_3$ UV absorption cross sections

The $CBrF_3$ cross sections obtained in this work at 9 discrete wavelengths from 195 to 235 nm and at temperatures over the range 210 to 320 K are given in Table 1. Our 296 K data is shown in Fig. 1 along with results from previous studies. At all wavelengths and temperatures, the absorption measurements obeyed Beer's

Table 1
$CBrF_3$ (Halon-1301) absorption cross sections, $\sigma(\lambda,T)$ (base e), measured in this work.[a]

λ (nm)	σ(λ,T) (10^{-20} cm^2 molecule^{-1}, base e)					
	320 K	296 K	270 K	250 K	230 K	210 K
195	9.07 ± 0.02	9.25 ± 0.01	9.57 ± 0.04	9.79 ± 0.04	10.08 ± 0.03	10.36 ± 0.03
200	11.26 ± 0.03	11.62 ± 0.02	12.14 ± 0.03	12.42 ± 0.04	12.80 ± 0.02	13.14 ± 0.05
205	12.48 ± 0.03	12.88 ± 0.02	13.41 ± 0.03	13.83 ± 0.06	14.28 ± 0.02	14.74 ± 0.05
210	12.01 ± 0.03	12.35 ± 0.03	12.81 ± 0.07	13.20 ± 0.05	13.62 ± 0.08	14.1 ± 0.1
215	10.17 ± 0.05	10.36 ± 0.02	10.67 ± 0.06	10.86 ± 0.03	11.10 ± 0.04	11.39 ± 0.05
220	7.61 ± 0.02	7.62 ± 0.02	7.68 ± 0.04	7.79 ± 0.03	7.88 ± 0.06	7.93 ± 0.03
225	5.09 ± 0.02	4.98 ± 0.01	4.91 ± 0.01	4.86 ± 0.03	4.80 ± 0.01	4.74 ± 0.02
230	3.097 ± 0.006	2.906 ± 0.009	2.770 ± 0.007	2.66 ± 0.02	2.521 ± 0.007	2.43 ± 0.02
235	1.705 ± 0.005	1.557 ± 0.005	1.410 ± 0.006	1.289 ± 0.007	1.180 ± 0.009	1.090 ± 0.006

[a] Quoted uncertainties are the 2σ precision values from the Beer's law fit of the experimental data. In some cases, the least significant digit may not be statistically significant, but was included to represent the precision of the fit.

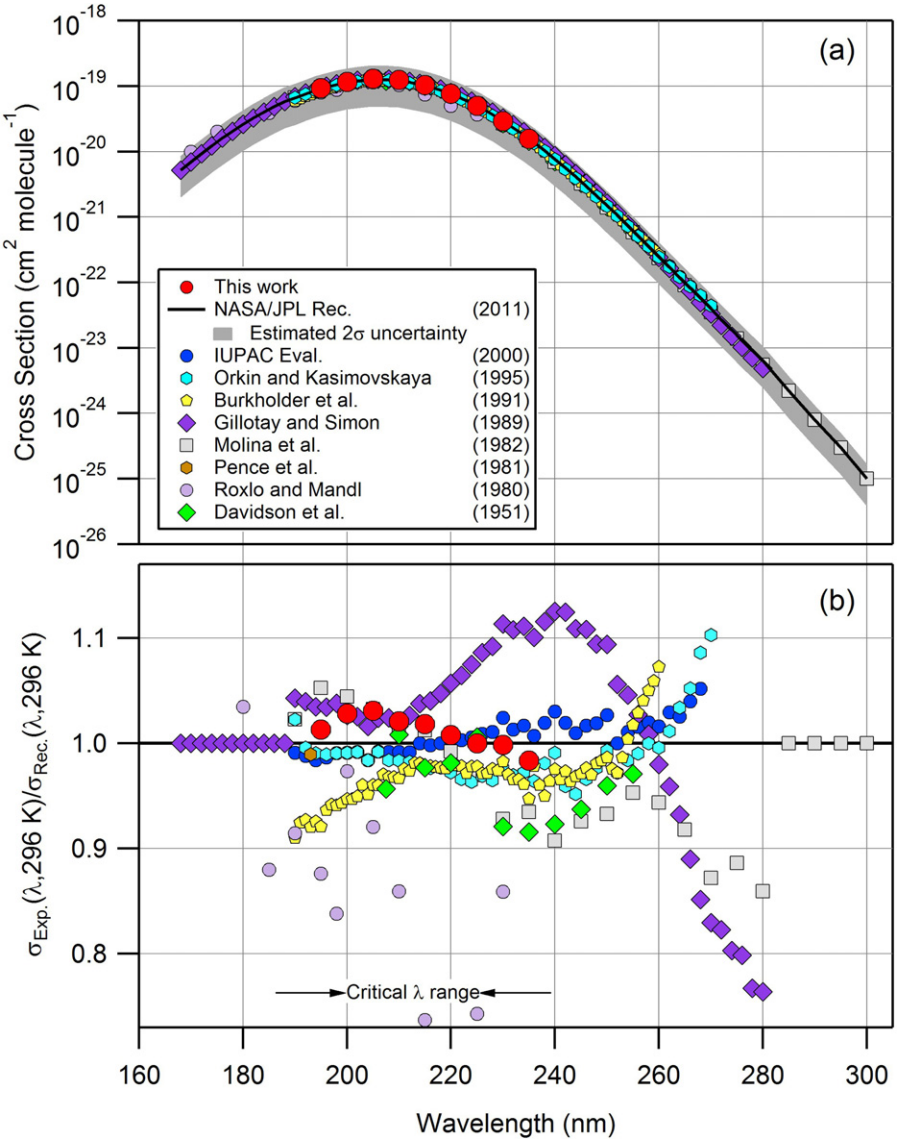

Fig. 1. Compilation of $CBrF_3$ (Halon-1301) room temperature UV absorption spectrum data. Panel (a): results from this work and previously published studies (see legend). The NASA/JPL recommended spectrum and its estimated 2σ uncertainty is included for comparison [5]. Panel (b) illustrates the spread in the available data relative to the NASA/JPL recommendation [5].

law over a wide concentration range, $(0.015\ to\ 5.1) \times 10^{17}$ molecule cm^{-3}. The experimental data obtained at each wavelength and temperature is provided graphically in the supplementary material, Fig. S1. The agreement among independent measurements was very good, to within 1%, and the final $\sigma(\lambda,T)$ values were obtained from a linear least-squares fit of all data obtained for the same temperature and wavelength.

A $CBrF_3$ cross section dependence on temperature was observed at all wavelengths included in this study. The temperature dependence at each wavelength is displayed in Fig. 2 relative to $\sigma(\lambda,296\ K)$. For the range of temperatures included in this study, the $CBrF_3$ cross sections at wavelengths $\leq$220 nm increased with decreasing temperature. The temperature dependence for wavelengths $\leq$220 nm was greatest at 205 nm where σ(205 nm,T) increased ~18% between 210 and 320 K. At wavelengths >220 nm, $\sigma(\lambda,T)$ decreased with decreasing temperature with the largest dependence observed at the longest wavelength, where σ(235 nm, T) decreased ~55% between 210 and 320 K. The cross section data obtained at each wavelength is also provided graphically in the supplementary material, Fig. S2.

4.2. Uncertainty analysis

Overall, the measurement precision of the measurements was very good, i.e., better than 1%, with the uncertainty at the longer wavelengths being slightly greater. The uncertainties reported in Table 1 are the precision of a linear least-squares fit of the experimental data to equation 1. Possible systematic errors in the measured pressure, temperature, sample mixing ratio, optical pathlength, and measured absorbance (and range) contribute to the estimated overall absolute uncertainty in $\sigma(\lambda,T)$ and are discussed below.

The uncertainties in the optical pathlength and the sample mixing ratio are ~0.5%, or less. The temperature uncertainty in the absorption cell was estimated to be 2 K at 210 K and 1 K for higher temperatures. The uncertainty in the absorption cell temperature primarily impacts the $CBrF_3$ concentration determination, as the absorption spectrum is not overly sensitive to uncertainties of 1 to 2 K. The uncertainty in the cell pressure and the linearity of the pressure measurement were estimated to be 0.2%. The stability of the light source lamp was ~0.3% at all wavelengths used in this

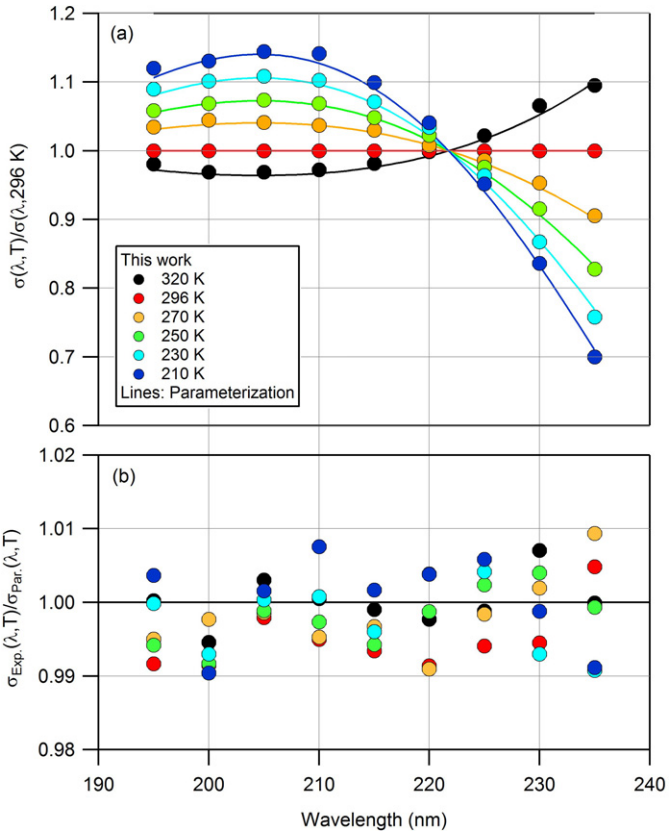

Fig. 2. Compilation of the $CBrF_3$ (Halon-1301) UV absorption cross section data obtained in this work between 210 and 320 K (see Table 1). Panel (a) the spectrum temperature dependence (see legend) relative to the room temperature spectrum, $\sigma(\lambda,T)/\sigma(\lambda,296\,K)$. The lines are the ratios obtained using the spectrum parameterization given in Table 2. Panel (b) shows the quality of the parameterization derived in this work in terms of the ratio of the experimental data to the spectrum parameterization.

study and I_0 measured before and after an experiment agreed to within 0.5%. The before and after I_0 values were averaged in the data analysis.

Independent experiments performed with different dilute mixtures of $CBrF_3$ as well as different $CBrF_3$ samples agreed to better than 1.5% (the majority of our sensitivity measurements were performed at 210 nm). Seven independent measurements were performed at 210 nm and 296 K. The measurements included variations in the optical setup, $CBrF_3$ samples with three different bulb mixing ratios, and two different $CBrF_3$ samples. The agreement among the measurements was better than 1.5%. Replicate measurements performed at other wavelengths and temperatures showed a comparable level of agreement, see Fig. S1. The overall absolute uncertainty in σ(λ,T) was estimated to be ~3% over the entire range of wavelengths and temperatures included in this work. Note that the cross section trends with temperature obtained at each specific wavelength are expected to be more accurate than the absolute values. The present high precision and rigorously tested measurement results supersede the results from Burkholder et al. [7] between 195 and 235 nm.

4.3. $CBrF_3$ UV spectrum parameterization

The σ(λ,T) data given in Table 1 was parameterized using the empirical formula given in Table 2. The calculated spectra are included in Fig. 2 for comparison with the experimental data; the experimental data is reproduced to within 1% at all wavelengths and temperatures. The parameterization is only valid over the wavelength and temperature range of the experimental data obtained in this study and extrapolation outside this range may lead to systematic error.

Table 2
$CBrF_3$ (Halon-1301) absorption cross section, $\sigma(\lambda,T)$, parameterization derived from the data in this work. The parameterization is valid over the range of the measurements, 195–235 nm and 210–320 K. The units of $\sigma(\lambda,T)$ are cm^2 $molecule^{-1}$ (base e), wavelength, λ, is in nanometer (nm), and the temperature, T, is in Kelvin (K).

$$\ln(\sigma(\lambda,T)) = \sum_{i=0}^{4} A_i\lambda^i + (T-296)\times\sum_{i=0}^{4} B_i\lambda^i$$

i	A_i	B_i
0	315.204	0.0077
1	-8.03836	-5.6975×10^{-4}
2	0.06362234	1.1304×10^{-5}
3	-2.1356×10^{-4}	-7.3977×10^{-8}
4	2.5779×10^{-7}	1.5279×10^{-10}

4.4. Comparison with previous $CBrF_3$ spectrum studies

4.4.1. Room temperature data

The room temperature results obtained in the present work are in agreement with results from previous studies recommended in the NASA/JPL data evaluation [5]. A comparison of the room temperature spectra is included in Fig. 1. A thorough discussion of the previous studies is provided in the NASA/JPL data evaluation [5] and is not repeated here. The NASA/JPL recommendation is also included in Fig. 1 for comparison. Results from the studies of Eden et al. [8], and Doucet et al. [15] differ significantly from the other studies and were not considered in the recommendation. The NASA/JPL recommendation was based on the data of Gillotay and Simon [6] in the region 168-188 nm, the mean of the Molina et al. [16], Gillotay and Simon [6], Burkholder et al. [7], and Orkin and Kasimovskaya [17] data between 190 and 270 nm, and the mean of the Molina et al. [16], Gillotay and Simon [6], and Burkholder et al. [7] data between 272 and 280 nm. Our room temperature spectrum is slightly, ~3%, greater than the NASA/JPL recommendation over the wavelength region 195-220 nm. Note, however, that the spread in the data from the previous studies is 10%, or less, over this wavelength region.

The uncertainty recommended in the NASA/JPL evaluation of 30% (1σ) is for the product of the $CBrF_3$ absorption spectrum and its photolysis quantum yield [5]. The NASA/JPL evaluation also recommends a $CBrF_3$ quantum yield of unity. Therefore, the recommended uncertainty is primarily due to the uncertainty in the absorption spectrum. The estimated uncertainty, however, far exceeds the spread in the available room temperature data in the 195-235 nm spectral region. A conclusion from our study is that a more appropriate uncertainty estimate for σ(195-235 nm,296 K) would be 5% (2σ).

4.4.2. Temperature dependence measurement

Two previous studies reported the temperature dependence of the $CBrF_3$ spectrum, Gillotay and Simon [6] (210-295 K, 168-280 nm) and Burkholder at al. [7] (210-296 K, 190-285 nm). The two studies differ with respect to the spectrum temperature dependence at wavelengths <210 nm and the magnitude of the spectrum temperature dependence at all wavelengths <235 nm. The NASA/JPL evaluation does not make an explicit recommendation for the $CBrF_3$ spectrum temperature dependence [5], while the IUPAC evaluation [18] recommends the mean of values of Gillotay and Simon [6] and Burkholder et al. [7] at 210 K. The spectrum

parameterization of Burkholder at al. [7] was recommended in the SPARC lifetime evaluation [1].

The parameterization of σ(λ,T) developed in this work for the wavelength range 195 to 235 nm is compared with the experimental data of Gillotay and Simon [6] and Burkholder et al. [7] in Fig. 3. The differences between these studies and the present work are systematic and outside the estimated uncertainty in the present work. Burkholder et al. [7] reported a relatively weak temperature dependence below 215 nm, whereas Gillotay and Simon [6] reported an increase in σ(λ,T) with decreasing the temperature of about 18% at 200 nm between 210 and 295 K. The present σ(λ,T) results display a temperature dependence that is intermediate between the two previous studies. The impact of the present σ(λ,T) results on the uncertainty in atmospheric photolysis rates, local and global lifetimes, and ODPs is quantified in Section 4.5.

4.5. Atmospheric implications

The present results were used in the GSFC 2-D atmospheric model to calculate globally annually averaged atmospheric lifetimes and the ozone depletion potential (ODP) of $CBrF_3$ for year 2000 steady-state conditions. The model has been used extensively in previous studies to quantify the atmospheric loss processes of ODSs and replacement compounds [1,11,13,19]. For this work, we evaluated the atmospheric impacts of the $CBrF_3$ photolytic loss at 195–235 nm using the absorption cross section parameterization given in Table 2. The Lyman-α cross section, 2.5×10^{-17} cm^2 $molecule^{-1}$, and UV cross sections at wavelengths less than 195 nm and greater than 235 nm were taken from SPARC [1]. A unit photolysis quantum yield at all wavelengths was assumed in the calculations. The $O(^1D)$, OH, and Cl reactive rate coefficients for $CBrF_3$ were also taken from SPARC [1]. We note that the $CBrF_3$ photolytic and reactive loss parameters from SPARC [1] are identical to those given in the NASA/JPL evaluation [5], with the exception of the Cl atom reactive loss, which was not included in the NASA/JPL recommendation. However, reaction with Cl atoms is a negligible loss process for $CBrF_3$ as discussed below. Kinetic and photochemical parameters for all other compounds were taken from the NASA/JPL evaluation [5] unless updated in SPARC [1].

The calculated fractional contributions to the atmospheric loss of $CBrF_3$ are given in Table 3. The photolytic loss was divided into 5 wavelength regions, the VUV at Lyman-α (121.567 nm) and in the UV wavelength regions 169–190, 190–230, 230–286, and >286 nm. The contributions due to reactive loss with $O(^1D)$, OH, and Cl atoms are also shown. Fig. 4 shows the calculated local altitude dependent contributions to the loss of $CBrF_3$. Table 3 and Fig. 4 clearly show that UV photolysis at 190–230 nm is the predominant loss process for $CBrF_3$ above ~10 km. The calculated molecular loss rates and $CBrF_3$ mixing ratio vertical profile are also included in

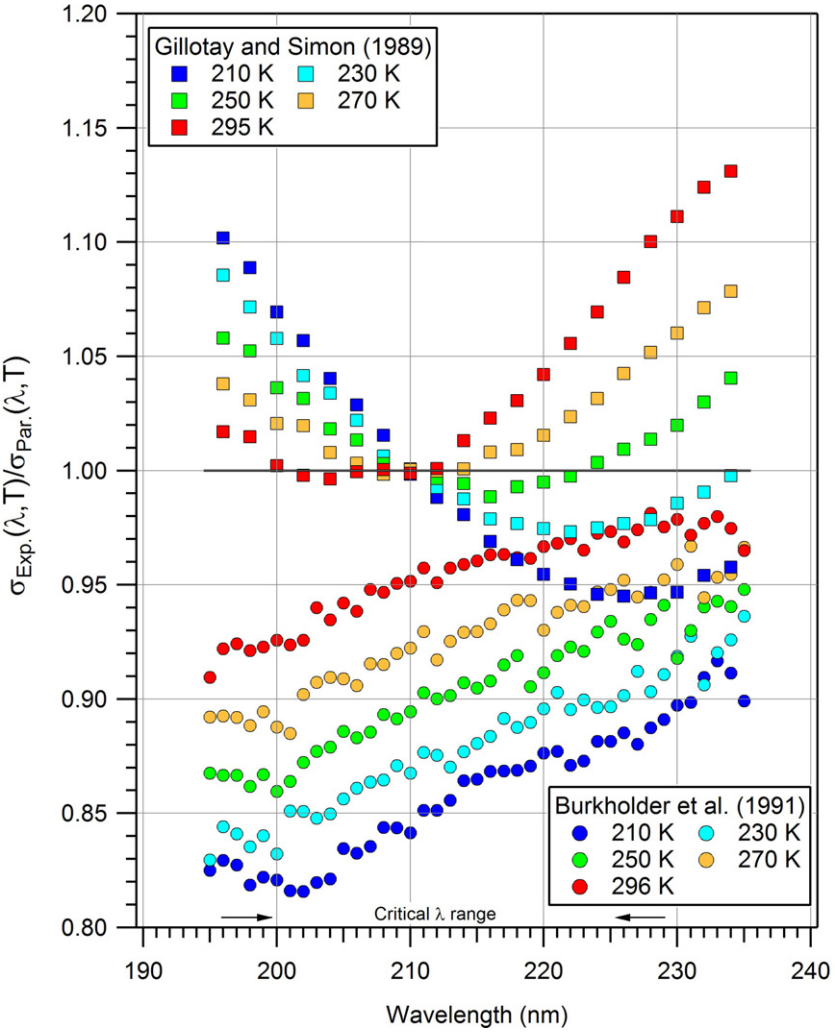

Fig. 3. Comparison of the $CBrF_3$ UV absorption spectra obtained in the present study with the results from previous studies of the spectrum temperature dependence expressed as the ratio of the experimental data to the parameterization developed in this work (see Table 2).

Table 3
Fractional contributions of photolysis and reactive processes to the atmospheric loss for $CBrF_3$ (Halon-1301) calculated using the GSFC 2-D atmospheric model.

Atmospheric loss process	Fractional contribution to total loss
Photolysis loss regions	
Lyman-α (121.567 nm)	<0.001
169-190 nm	<0.001
190-230 nm	0.987
230-286 nm	<0.001
>286 nm	0.002
Total	0.989
Reactive loss processes	
$O(^1D)$	0.006
OH	<0.004
Cl	<0.001

Fig. 4. The maximum molecular loss rate of $CBrF_3$ is near 25 km with significant loss rates over the altitude range 18–31 km. This altitude range corresponds to a temperature range between ~205 and 230 K, i.e., the temperature range over which $\sigma(\lambda,T)$ is most critical. The calculated vertical mixing ratio shows that >99% of $CBrF_3$ is removed below 32 km.

The $CBrF_3$ lifetime was computed as the ratio of the annually averaged global atmospheric burden to the vertically integrated annually averaged total global loss rate [1]. The total global lifetime can be separated by the troposphere (surface to the tropopause, seasonally and latitude-dependent), stratosphere, and mesosphere (<1 hPa) using the total global atmospheric burden and the loss rate integrated over the different atmospheric regions such that

$$\frac{1}{\tau_{\text{Total}}} = \frac{1}{\tau_{\text{Trop}}} + \frac{1}{\tau_{\text{Strat}}} + \frac{1}{\tau_{\text{Meso}}}$$

Using the cross sections reported in this work, the global annually averaged lifetime for $CBrF_3$ was calculated to be 74.6 years, and the lifetimes for the various atmospheric regions are given in Table 4. As indicated in Table 3, UV photolysis in the wavelength region 190–230 nm accounts for nearly 99% of the total global atmospheric loss of $CBrF_3$. The vast majority of $CBrF_3$ is removed in the stratosphere with tropospheric removal accounting for ~2.5% of the total loss. Although Lyman-α photolysis is a dominant mesospheric loss process, the contribution of mesospheric loss to the global lifetime is negligible. Long-wavelength UV photolysis, $\lambda > 290$ nm, makes a minor contribution to the stratospheric photolysis loss at all altitudes. Reaction with $O(^1D)$ is also a minor stratospheric loss process and accounts for ~0.6% of the total $CBrF_3$ loss. Note that both UV photolysis and the $O(^1D)$ reaction lead to the formation of stratospheric reactive bromine in the form of Br atoms and BrO radicals, respectively, i.e., both loss processes initiate the depletion of stratospheric ozone. In the troposphere, loss by reaction with the OH radical (using the NASA/JPL recommended reaction rate coefficient upper-limit in the model calculations) is a negligible loss process, <0.4%. Long-wavelength photolysis in the troposphere primarily accounts for the 3000 year tropospheric lifetime given in Table 4.

As indicated in Table 4, the total lifetime using only the room temperature spectrum was calculated to be 76.7 years. Therefore, including the temperature dependence of the $CBrF_3$ UV absorption spectrum in the calculation leads to a decrease of 2.1 years (3%) in the atmospheric lifetime.

The GSFC 2-D atmospheric model calculated a globally annually averaged lifetime of 74.6 ± 0.9 years for this work, compared with $77.4 \pm$ ~7 years for SPARC [1] and $77.4 \pm$ ~10 years for NASA/JPL [5] (see Table 4). The lower uncertainty in the atmospheric lifetime reported in this work is due to the smaller uncertainty on the absorption cross section (±5%, 2σ) compared to SPARC (±8%, 2σ) and NASA/JPL (±30%, 1σ). The computed atmospheric lifetime is reduced by ~3 years for this work, due to the slightly greater UV absorption cross sections in the 195–235 nm wavelength range.

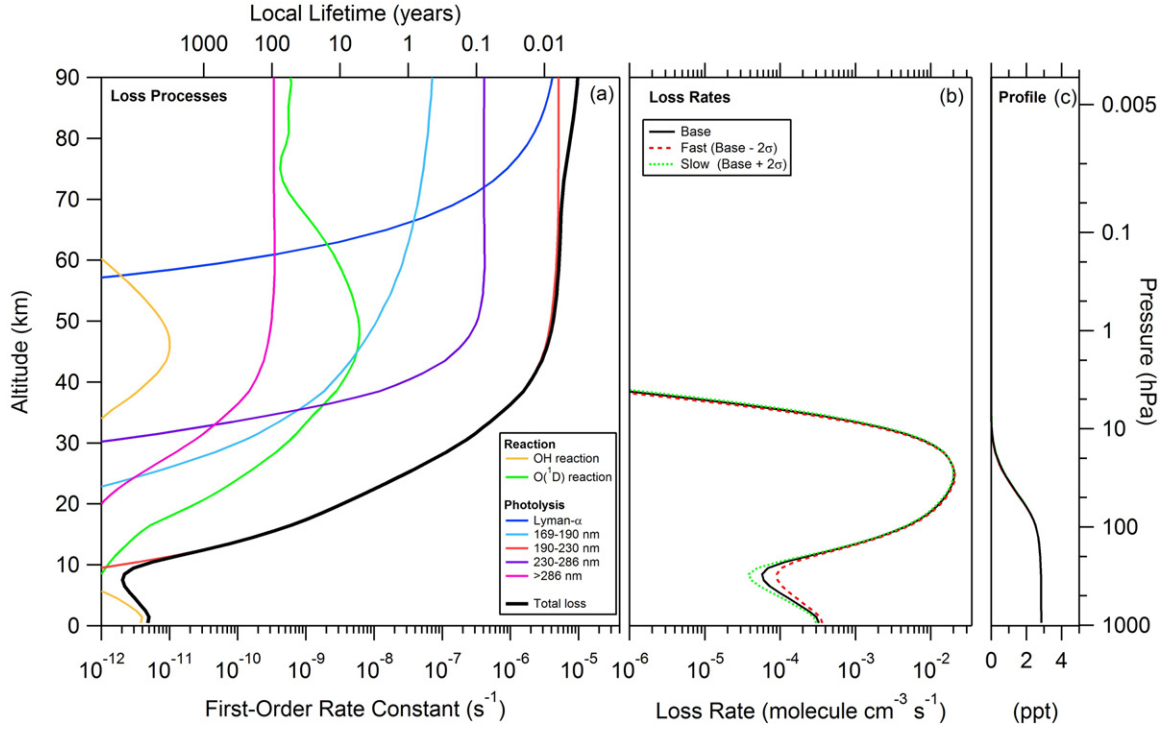

Fig. 4. 2-D atmospheric model results for $CBrF_3$ (Halon-1301). (a) Loss rate coefficients (local lifetimes) combining the photolysis and reaction processes. (b) Molecular loss rates and uncertainty limits: slow and fast profiles calculated using the uncertainty on the UV absorption spectrum of $CBrF_3$ obtained in this work. (c) Mixing ratio vertical profile of $CBrF_3$.

Table 4
Globally annually averaged atmospheric lifetimes of $CBrF_3$ (Halon-1301) calculated using the GSFC 2-D model for 2000 steady-state conditions and ozone depletion potentials (ODP) from this work, SPARC [1], and NASA/JPL [5].

	Lifetime (years)		
	This work	SPARC	NASA/JPL
Tropospheric	3000	3340	3340
Stratospheric	76.5	79.3	79.3
Mesospheric	$>1\times10^6$	$>1\times10^6$	$>1\times10^6$
Total	74.6 (73.7-75.5)[a]	77.4 (72.9-81.8)[a]	77.4 (68.7-86.5)[a]
	±1.2%	±6%	±11.5%
Total (296 K spectrum only)	76.7		
	Ozone depletion potential		
	This work	SPARC	NASA/JPL
2-D model	18.6 (18.5–18.6)[b]	18.3 (18.0–8.6)[b]	18.9 (18.0–19.4)[b]
Semi-empirical[c]	15.7 (15.6–15.9)	16.3 (15.4–17.3)	16.3 (14.5–18.3)
Semi-empirical[d]	19.7 (19.5–19.9)	20.4 (19.2–21.6)	20.4 (18.1–22.8)

[a] The values in parenthesis are the range of lifetimes calculated using the estimated 2σ high and low values of the $CBrF_3$ UV absorption spectrum at 190–230 nm reported in the individual reports and in this work.
[b] The values in parenthesis are the range of ODPs calculated with the 2-D model using the estimated 2σ high and low values of the $CBrF_3$ UV absorption spectrum between 190 and 230 nm reported in the individual reports and in this work.
[c] Based on fractional release factors in WMO [2,3].
[d] Based on fractional release factors in Laube et al. [20] with a mean age of air of 3 years.

We also examined the impact of the present UV absorption cross section data on the determination of the ozone depletion potential (ODP), determined both semi-empirically and calculated in the 2-D model. The semi-empirical ODP for $CBrF_3$ (Halon-1301) was calculated relative to $CFCl_3$ (CFC-11) using the method outlined in WMO [3]

$$\mathrm{ODP} = (\alpha \times n_{\mathrm{Br}}) \times \frac{\mathrm{FRF}_{\mathrm{Halon-1301}}}{\mathrm{FRF}_{\mathrm{CFC-11}}} \times \frac{\tau_{\mathrm{Halon-1301}}}{\tau_{\mathrm{CFC-11}}} \times \frac{M_{\mathrm{CFC-11}}}{M_{\mathrm{Halon-1301}}} \times \frac{1}{3}$$

with α, the relative ozone destruction effectiveness of bromine compared to chlorine ($\alpha = 60$ [2]), n_{Br} is the number of bromine atoms, FRF is the fractional release factor, τ is the global atmospheric lifetime and M is the molar mass.

The global atmospheric lifetime of CFC-11 was taken to be 52 years as in SPARC [1] and WMO [3]. For comparison, two sets of fractional release factors for $CBrF_3$ and CFC-11 are used: 0.28 and 0.47, respectively, as in WMO [3], and 0.26 and 0.35, respectively as in Laube et al. [20] using a mean age of air of 3 years. Using these two sets of fractional release factors, semi-empirical ODPs were obtained using global atmospheric lifetimes computed from this work, the SPARC, and NASA/JPL parameters and are presented in Table 4. For the $CBrF_3$ lifetimes obtained in this work, the semi-empirical ODP ranges from 15.7 to 19.7 for the two sets of fractional release factors. For comparison, we also show ODPs calculated directly from the 2-D model as both semi-empirical and model-base ODPs are used in the WMO [2,3] assessment reports. Using the $CBrF_3$ loss parameters from this work, the 2-D model calculated ODP of 18.6 falls between the semi-empirical ODPs, illustrating that the 2-D model and semi-empirical approach are in general agreement considering the uncertainties on the global atmospheric lifetime and the fractional release factors.

For both methods, Table 4 also shows the range in ODPs obtained using the 2σ high and low uncertainty on the UV absorption cross sections between 195 and 235 nm from this work, SPARC [1], and NASA/JPL [5]. This illustrates that for both the model-based and semi-empirical ODPs, the uncertainty range in ODPs is significantly reduced in this work ($< \pm 1\%$), vs. the spectrum uncertainties from SPARC (±2–6%) and NASA/JPL (±4–12%).

5. Conclusion

In summary, high-precision measurements of $\sigma(\lambda,T)$ for $CBrF_3$ over the wavelength and temperature ranges most critically important for atmospheric photolysis were presented in this work. Atmospheric model calculations have shown that short-wavelength UV photolysis is the predominant atmospheric loss process for $CBrF_3$. It was also shown that the 190–230 nm wavelength range accounts for the vast majority of photolysis. The global lifetime of $CBrF_3$ was calculated to be 74.6 years ± 1.2%. While the lifetime obtained in this work is similar to that reported in previous evaluations [1] the possible range of lifetimes and associated ODPs due solely to the uncertainty in $\sigma(\lambda,T)$ were significantly reduced. It would also be expected that because of the variation in model treatment of atmospheric processes, the variation in lifetimes and ODPs among different models would be greater than that due to the cross section uncertainty.

Acknowledgements

This work was supported in part by NOAA's Atmospheric Chemistry, Carbon Cycle, and Climate (AC4) Program and NASA's Atmospheric Composition Program.

Appendix A. Supplementary data

Supplementary data associated with this article can be found, in the online version, at http://dx.doi.org/10.1016/j.jphotochem.2015.03.012.

References

[1] SPARC report on lifetimes of stratospheric ozone-depleting substances, their replacements, and related species, M., Ko, P., Newman, S., Reimann, S. Strahan (Eds), SPARC Report No. 6, WCRP-15/2013, 255 pp., 2013, http://www.sparc-climate.org/publications/sparc-reports/sparc-report-no6/.
[2] WMO. (World Meteorological Organization), Scientific Assessment of Ozone Depletion: 2010, Global Ozone Research and Monitoring Project – Report No. 52, 516 pp., Geneva, Switzerland, 2011, http://www.wmo.int/pages/prog/arep/gaw/ozone_2010/documents/Ozone-Assessment-2010-complete.pdf.
[3] WMO (World Meteorological Organization), Scientific Assessment of Ozone Depletion. 2014, Global Ozone Research and Monitoring Project – Report No. 55, 416 pp., Geneva, Switzerland, 2014, http://www.wmo.int/pages/prog/arep/gaw/ozone_2014/ozone_asst_report.html.
[4] M.J. Newland, C.E. Reeves, D.E. Oram, J.C. Laube, W.T. Sturges, C. Hogan, P. Begley, P.J. Fraser, Southern hemispheric halon trends and global halon emissions, 1978–2011, Atmos. Chem. Phys. 13 (2013) 5551–5565.
[5] S.P. Sander, J. Abbatt, J.R. Barker, J.B. Burkholder, R.R. Friedl, D.M. Golden, R.E. Huie, C.E. Kolb, M.J. Kurylo, G.K. Moortgat, V.L. Orkin, P.H. Wine, Chemical Kinetics and Photochemical Data for Use in Atmospheric Studies, Evaluation

No. 17, JPL Publication 10-6, Jet Propulsion Laboratory, Pasadena, 2011. . 684 pp. http://jpldataeval.jpl.nasa.gov.
[6] D. Gillotay, P.C. Simon, Ultraviolet absorption spectrum of trifluoro-bromo-methane, difluoro-dibromo-methane and difluoro-bromo-chloro-methane in the vapor phase, J. Atmos. Chem. 8 (1989) 41–62.
[7] J.B. Burkholder, R.R. Wilson, T. Gierczak, R. Talukdar, S.A. McKeen, J.J. Orlando, G.L. Vaghjiani, A.R. Ravishankara, Atmospheric fate of CF_3Br, CF_2Br_2, CF_2ClBr, and CF_2BrCF_2, Br. J. Geophys. Res. 96 (1991) 5025–5043.
[8] S. Eden, P. Limão-Vieira, S.V. Hoffmann, N.J. Mason, VUV photoabsorption in CF_3X (X = Cl, Br, I) fluoro-alkanes, Chem. Phys. 323 (2006) 313–333.
[9] E.L. Fleming, C.H. Jackman, D.K. Weisenstein, M.K.W. Ko, The impact of interannual variability on multidecadal total ozone simulations, J. Geophys. Res 112 (2007) D10310.
[10] E.L. Fleming, C.H. Jackman, R.S. Stolarski, A.R. Douglass, A model study of the impact of source gas changes on the stratosphere for 1850–2100, Atmos. Chem. Phys. 11 (2011) 8515–8541.
[11] M.R. McGillen, E.L. Fleming, C.H. Jackman, J.B. Burkholder, $CFCl_3$ (CFC-11): UV absorption spectrum temperature dependence measurements and the impact on its atmospheric lifetime and uncertainty, Geophys. Res. Lett. 40 (2013) 4772–4776.
[12] V.C. Papadimitriou, M.R. McGillen, E.L. Fleming, C.H. Jackman, J.B. Burkholder, NF_3: UV absorption spectrum temperature dependence and the atmospheric and climate forcing implications, Geophys. Res. Lett. 40 (2013) 440–445.
[13] N. Rontu Carlon, D.K. Papanastasiou, E.L. Fleming, C.H. Jackman, P.A. Newman, J.B. Burkholder, UV absorption cross sections of nitrous oxide (N_2O) and carbon tetrachloride (CCl_4) between 210 and 350 K and the atmospheric implications, Atmos. Chem. Phys. 10 (2010) 6137–6149.
[14] S.W. Sharpe, T.J. Johnson, R.L. Sams, P.M. Chu, G.C. Rhoderick, P.A. Johnson, Gas-phase databases for quantitative infrared spectroscopy, Appl. Spectrosc. 58 (2004) 1452–1461.
[15] J. Doucet, P. Sauvageau, C. Sandorfy, Vacuum ultraviolet and photoelectron spectra of fluoro-chloro derivatives of methane, J. Chem. Phys. 58 (1973) 3708–3716.
[16] L.T. Molina, M.J. Molina, F.S. Rowland, Ultraviolet absorption cross sections of several brominated methanes and ethanes of atmospheric interest, J. Phys. Chem. 86 (1982) 2672–2676.
[17] V.L. Orkin, E.E. Kasimovskaya, Ultraviolet absorption spectra of some Br-containing haloalkanes, J. Atmos. Chem. 21 (1995) 1–11.
[18] R. Atkinson, R.A., Cox J.N., Crowley, M.E., Jenkin, A., Mellouki, M.J., Rossi, J., Troe, T.J. Wallington, IUPAC Task Group on Atmospheric Chemical Kinetic Data Evaluation, http://iupac.pole-ether.fr.
[19] V.C. Papadimitriou, M.R. McGillen, S.C. Smith, A.M. Jubb, R.W. Portmann, B.D. Hall, E.L. Fleming, C.H. Jackman, J.B. Burkholder, 1,2-Dichlorohexafluoro-cyclobutane (1,2-c-C4F6Cl2, R-316c) a potent ozone depleting substance and greenhouse gas: atmospheric loss processes, lifetimes, and ozone depletion and global warming potentials for the (*E*) and (*Z*) stereoisomers, J. Phys. Chem. A 117 (2013) 11049–11065.
[20] J.C. Laube, A. Keil, H. Bönisch, A. Engel, T. Röckmann, C.M. Volk, W.T. Sturges, Observation-based assessment of stratospheric fractional release, lifetimes, and ozone depletion potentials of ten important source gases, Atmos. Chem. Phys. 13 (2013) 2779–2791.